Temperature dependence of chemical exchange during seafloor weathering: insights from the Troodos ophiolite

Laurence A. Coogan, K.M. Gillis

2018

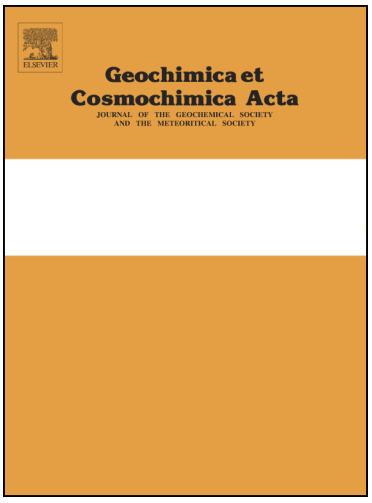

Temperature dependence of chemical exchange during seafloor weathering: Insights from the Troodos ophiolite

L.A. Coogan, K.M. Gillis

PII: S0016-7037(18)30550-7
DOI: https://doi.org/10.1016/j.gca.2018.09.025
Reference: GCA 10948

To appear in: *Geochimica et Cosmochimica Acta*

Received Date: 1 May 2018
Revised Date: 18 September 2018
Accepted Date: 22 September 2018

Please cite this article as: Coogan, L.A., Gillis, K.M., Temperature dependence of chemical exchange during seafloor weathering: Insights from the Troodos ophiolite, *Geochimica et Cosmochimica Acta* (2018), doi: https://doi.org/10.1016/j.gca.2018.09.025

Temperature dependence of chemical exchange during seafloor weathering: insights from the Troodos ophiolite

[1]L.A. Coogan and [1]K.M. Gillis

[1]School of Earth and Ocean Sciences, University of Victoria, Victoria, BC, Canada

[*]Corresponding author: lacoogan@uvic.ca, tel: (1)250 472 4018

Submitted to Geochimica et Cosmochimica Acta 1st May 2018

Revised and returned 18th Sept. 2018

ABSTRACT

Chemical fluxes associated with low-temperature, off-axis, alteration of the upper oceanic crust (seafloor weathering) may play an important role in controlling the composition of the ocean and the long-term carbon cycle. However, it is challenging to quantify these fluxes and how they change with changing bottom water temperature over geological timescales. Here we study the exchange of major elements associated with seafloor weathering in the exceptionally preserved Cretaceous Troodos ophiolite and compare them to less well constrained data from drill cores from the modern ocean basins. Calcite O-isotope thermometry from four traverses through the lavas reveals a well-ventilated region at the top of the lava pile where alteration occurred at near-constant temperatures similar to that of bottom water. The lithological makeup of the crust appears to control the thickness of this region, with increased abundance of sheet flows marking the base of this zone. Maintaining low-temperatures in the well-ventilated region requires large fluid fluxes facilitated by the high permeability of the pillow lavas. Large-scale addition of CO_2 to the crust only occurs in this well-ventilated region indicating that the alkalinity producing reactions required for calcite precipitation occurred at temperatures sensitive to bottom water temperature. Comparison of whole rock geochemical data for samples from the well-ventilated zone with volcanic glass compositions shows that the changes in rock compositions due to seafloor weathering are large (roughly -4 wt% SiO_2, +0.5 to 1 wt% MgO, -5 wt% CaO, -0.5 wt% Na_2O, +3.5 wt% K_2O and + 2.5 wt% CO_2). Comparison to data from drill cores from modern oceanic crust that was also altered under well-ventilated conditions suggests that bottom water temperature plays a major role in controlling the chemical exchange between the ocean and lavas; parameterizations for the associated fluxes are provided. Because elemental exchange between the ocean and oceanic crust globally depends strongly on bottom water temperature, fixed values for these fluxes cannot be used in models of the evolution of seawater chemistry or subduction fluxes.

1. INTRODUCTION

The major ion composition of seawater is important in many aspects of the Earth system from its effect on the carbon cycle (via alkalinity) to modulating biomineralization (e.g. Sundquist, 1991; Porter, 2010). Additionally, because the major ion composition of the ocean reflects the integrated fluxes of ions into and out of the ocean, an understanding of the controls on ocean chemistry, along with a history of ocean chemistry, may allow the history of these fluxes to be unraveled (e.g. Spencer and Hardie, 1991; Demicco et al., 2005). Of the fluxes that play important roles in controlling ocean chemistry, perhaps the least well-constrained is that associated with low-temperature alteration of the upper oceanic crust (lavas) in off-axis hydrothermal systems. These systems operate across the abyssal plains starting close to the ridge axis and continuing until sufficient sediment accumulates to inhibit significant fluid exchange between the oceans and crustal aquifer (i.e. the high porosity and permeability lavas; Stein and Stein, 1992; Mottl and Wheat, 1994; Hasterok, 2013).

Chemical fluxes associated with off-axis hydrothermal circulation can potentially be determined either from changes in fluid or rock compositions. If the average change in fluid composition in the crust and the total fluid flux could be determined, the chemical flux could be calculated. However, finding fluids venting off-axis is incredibly challenging and estimates of aquifer fluid compositions from sediment pore fluid profiles suggest local hydrological conditions lead to massive variability in fluid composition; this makes using these to determine global average aquifer fluid compositions very difficult. Alternatively, if the average change in rock composition induced by off-axis fluid-rock reaction can be determined, and the total mass of rock altered in such systems estimated, the chemical flux can be calculated. It is this latter approach we use here, and we discuss the system from the perspective of the time-integrated change in rock composition that, via mass balance, reflect time integrated fluxes into the ocean.

The principal controls on the time-integrated chemical fluxes associated with off-axis hydrothermal systems are the temperature of fluid-rock reaction, the fluid flux and the composition of seawater. The temperature of fluid-rock reaction depends both on bottom water temperature (Brady and Gislason, 1997; Gillis and Coogan, 2011; Coogan and Dosso, 2015; Krissansen-Totton and Catling, 2017) and the extent of heating of the fluid in the aquifer; the latter depends on hydrological conditions, in particular sediment cover and aquifer permeability (Fisher and Becker, 2000; Anderson et al., 2012; Winslow et al., 2016). The same hydrological parameters control the fluid flux. Bottom water chemistry is potentially important in controlling chemical exchange between the crust and ocean because, in general, fluid fluxes are sufficiently large that the fluid composition for many species is similar to seawater even after fluid-rock reaction (Wheat et al., 2017; Coogan and Gillis, 2018). Unraveling the relative roles of the different factors in controlling chemical fluxes between the ocean and crustal aquifer in off-axis hydrothermal systems is complex because of the heterogeneity of hydrological conditions, limited sampling, and generally poor recovery of modern lavas through drilling. However, if we are to understand the role of off-axis hydrothermal systems in the evolution of seawater chemistry it is important to attempt to quantify the chemical fluxes as functions of the controlling parameters.

The Troodos ophiolite, Cyprus, is perhaps the only ophiolite that preserves a typical low-temperature alteration history analogous to that found in drill cores from the

modern oceanic crust, being largely unaffected by obduction related overprinting or rapid early sedimentation (Gillis and Robinson,1988; Gillis and Robinson, 1990). It also allows us to explore the controls on chemical exchange during low-temperature alteration of the lavas in ways that are not possible in drill cores from the modern ocean basins due to good exposure over a wide area. Additionally, there is a high-recovery (>90%) drill core through the lavas (Gibson et al., 1991). The Troodos ophiolite was formed (91.6±1.4 Ma; Mukasa and Ludden, 1987) and altered (Gallahan and Duncan, 1994; Booij et al., 1995) in the late Cretaceous, a time of high global temperatures (Cramer et al., 2011; Friedrich et al., 2012). Because surface temperature and bottom water temperature are strongly correlated (Krissansen-Totton and Catling, 2017) this ophiolite provides a good example of crust altered under warm bottom water conditions. The sedimentary record preserves a history of initially very slow, deep marine, sedimentation (Bear, 1960) with shallow marine conditions (e.g. reefal limestones) appearing in the Miocene (e.g. Follows and Robertson, 1990) as the ophiolite was uplifted (i.e. well after low-temperature alteration occurred). The spreading rate the ophiolite formed at is uncertain, but the continuous sheeted dike complex, general lack of crustal dismemberment, and limited topography on the lava-sediment boundary suggest either an intermediate- to fast-spreading rate or a magma supply rate consistent with these spreading rates.

Here we use whole rock geochemistry and carbonate mineral O-isotope thermometry (henceforth referred to as calcite although definitive mineralogical tests have not been performed on all samples) to investigate chemical exchange between the ocean and upper oceanic crust in off-axis hydrothermal systems. We show that the region of the crust in which the aquifer was well-ventilated, such that the aquifer temperature was similar to that of bottom water, depends largely on the lithological characteristics of the crust. Using samples from this well-ventilated area, and assuming that cogenetic volcanic glasses define fresh-rock compositions, we quantify the magnitude of chemical exchange during low-temperature alteration in this setting. Comparison of these chemical changes to those from drill cores in modern ocean crust that also underwent alteration under well-ventilated conditions suggests that bottom water temperature plays a key role in controlling major element fluxes between the ocean and upper oceanic crust. This dependence of the extent of alteration of the well-ventilated region on bottom water temperature means that use of the term "seafloor weathering" to describe this process is appropriate in that it makes the link between the control of climate, through bottom water temperature, and the extent of chemical exchange.

2. ANALYTICAL METHODS

Whole rock samples were crushed in an agate planetary mill and major element compositions were determined by XRF, and LECO for C, at Acme labs, Vancouver (Supplementary Table S1; previously reported in Coogan et al., 2017). Additionally, major element compositions measured on the CY1/1A drill cores as part of the Cyprus Crustal Study Project are also used (Gibson et al., 1991). Many of these drill core samples were analysed in up to four different laboratories and the averages of the data reported for these samples were calculated and used. The portion of the calcium hosted in silicate phases (CaO_{sil}) was determined by correcting for Ca in calcite by assuming all C exists as $CaCO_3$ (i.e. $CaO_{sil} = CaO - (56/44)*CO_2$). Chromium and Ni were analysed by solution ICP-MS. After dissolution using a HF:HNO_3 mixture samples were analysed on

a Thermo X-Series ICP-MS at the University of Victoria using In as the internal standard and BIR-1, BHVO-2, BCR-2, JB-2 and JR-2 rock standards dissolved with the samples to calibrate. Drift was monitoured, and corrected for, using an in-house solution of similar composition to the samples that was analyzed at regular intervals during each analytical session. Volcanic glass was gently crushed by hand and apparently alteration-free portions were picked under a binocular microscope and then mounted in epoxy and polished for analysis. Major elements were determined by electron microprobe at The University of British Columbia using a Cameca SX-50 with a 20 µm beam diameter, 20 nA beam current and 20 kV accelerating voltage. Glass Cr and Ni concentrations were determined using a New Wave 213 nm laser linked to the same ICP as used for the solution analyses (Supplementary Table S2). A 90 µm spot and 10 Hz repetition rate were used and the ablated material was transported from the laser cell to the ICP-MS in He. Calibration used Ca as the internal standard (as determined by electron microprobe) and NIST 612 as the single calibration standard. Data quality was checked by repeated analysis of BCR-2G and multiple MPI-DING glasses (Supplementary Table S2). During both electron microprobe and ICP-MS analysis, effort was made to avoid areas of the glass that contained microphenocrysts, which are common. Calcite samples were crushed and washed in DI in an ultrasonic bath to remove dust. Optically clean grains were then hand-picked under a binocular microscope. These were crushed to homogenize the material and then analysed for O-isotopes at the University of British Columbia using a Delta PlusXL mass spectrometer in continuous flow mode (Supplementary Table S3).

3. RESULTS

3.1. Field constraints

We present data from four transects through the lava section of the northern flank of the Troodos ophiolite that come from a ~20 km east-west region (Fig. 1). Each study area has somewhat different geological and hence paleo-hydrological conditions allowing us to test the role of different parameters in controlling chemical exchange during off-axis hydrothermal circulation. The study sections include a paleo-seafloor topographic high (Mitsero seamount), a paleo-seafloor topographic low (Onophrious graben) and two sections from flat paleo-seafloor, one sampled in outcrop (Politico) and one from drill-core (CY1/1A in the Akaki area). This variation in seafloor topography, identified both by mapping and variations in basal sediment age and type, led to large variations in the timing of sediment accumulation from synchronous with ophiolite formation (Onophrious) to starting ~20 Myrs (Akaki and Politico) to >50 Myrs (Mitsero) after crustal accretion (Bear, 1960; Follows and Robertson, 1990). The sections also vary in their proportion of sheet and pillow flows (Fig. 2) which is expected to lead to variations in bulk-permeability, with pillow-dominated regions having higher permeability than sheet-dominated regions. Different distributions of pillows and sheets, along with variation in the paleo-seafloor topography and the associated variations in timing of sedimentation, mean the paleo-hydrology of these crustal sections was variable (e.g. Bach et al., 2004; Fisher et al., 2014). To help in understanding the paleo-hydrology, calcite amygdales (and occasional vugs and veins) were sampled (Fig. 1) and are used to constrain the temperature of fluid-rock reaction using calcite O-isotope thermometry (Fig. 2).

Whole rock samples were collected through the lavas in the four areas (Fig. 1). Sampling extended from the lava-sediment boundary downwards until either the abundance of dikes approached ~50% and/or the alteration mineralogy (e.g. laumontite) or existing calcite O-isotope data suggested elevated alteration temperatures. As well as depth transects, pairs of lava samples from the interior and rim of pillows and sheets were commonly collected to determine the variability in the extent of alteration within individual "cooling units". Additionally, we sampled zoning profiles across three adjacent pillows of different sizes, and the associated interpillow material (originally glass spalled off pillows and void space; Fig. S1), at an outcrop near the top of the Akaki section previously described in detail by Gillis and Sapp (1997). Protolith geochemistry and phenocryst content varies within the lavas with more primitive lavas and olivine phenocrysts being more common in the upper lavas than deeper in the lava pile (e.g. Bear, 1960), with more primitive and more evolved lavas commonly being intermixed. When sampling we avoided very olivine-rich regions (the rare picritic lavas and picritic bases of pillows) to minimize uncertainty in protolith composition due to olivine accumulation, and the maximum amount of olivine in any sample used here is estimated to be <5%. Volcanic glass was collected throughout the study area (Fig. 1) to define possible protolith compositions.

The geology and secondary mineral assemblages in each area are described in the supplementary material and summarized in Fig. 2. Briefly, as reported previously (Gillis and Robinson, 1985, 1990), calcite is the main void filling phase in the uppermost part of each section with the zeolites analcime and philipsite becoming more common with increasing depth in the lavas. In the deeper portions of the lavas studied here celadonite and chalcedony, along with the zeolites mordenite and clinoptilolite, become common. Potassium feldspar occurs as a replacement of plagioclase in the uppermost part of the crust and smectite and Fe-oxyhydroxides occur throughout but are more abundant at shallow depths into the crust (Gillis and Robinson, 1985, 1990).

3.2. Oxygen isotope thermometry and fluid flux estimates

Fluid flux and fluid temperature are key controls of the time-integrated chemical exchange associated with off-axis hydrothermal systems. Because the crust is bathed in fluid throughout its lifetime, from the rocks perspective the duration of fluid-rock reaction is generally the lifetime of the piece of crust. Fluid flux, as well as local hydrological conditions such as fluid recirculation and position on a flow path, controls the supply of fresh, reactive seawater and hence is key to the time integrated chemical fluxes between the ocean and crust. Individual batches of fluid may, of course, have short residence times in the crust leading to minimal changes in fluid composition (e.g. Wheat et al., 2017; Lauer et al., 2018) but this simply leads to these fluids being replaced, leading to a relatively larger fluid fluxes where fluid residence times are shorter. Temperature is key in both controlling fluid-rock reaction kinetics and thermodynamics. If fluid fluxes are small, and hence advective heat transport limited, the temperature of fluid-rock reaction should increase with depth in the crust roughly along a conductive geotherm. Strong vertical mixing within the crust could eradicate vertical temperature gradients even at low fluid fluxes but this would require the unlikely characteristics of high vertical permeability (and a thick aquifer) but low horizontal permeability. In contrast, if fluid fluxes are large, near bottom water temperatures would be maintained throughout the region of high fluid flux provided the sediment cover is thin and hence

does not provide a substantial thermal blanket. The temperature of fluid-rock reaction, at least those reactions that generate alkalinity driving calcite precipitation, is recorded in the O-isotope composition of hydrothermal calcite.

Calcite O-isotope thermometry shows that the hydrothermal fluid had a limited temperature range (~10 to ~25°C) throughout a variable thickness region at the top of the lava pile in all areas (Fig. 2; Supplementary Table S3). This range is close to the temperature of late Cretaceous bottom water (8-20°C; Cramer et al., 2011; Friedrich et al., 2012) indicating that the reactions that drove calcite precipitation within this upper zone occurred at temperatures close to that of bottom water. Importantly, this region of low-temperature calcite precipitation shows no systematic change in temperature with depth (Fig. 2) indicating efficient thermal homogenization by advection of seawater; this is referred to here as the "well-ventilated" region (or, equivalently, the seafloor weathering zone). This region ranges in thickness from ~80-100 m (Onophrious) to ~300 m (Akaki; Fig. 2; cf. Gillis and Robinson, 1990; Gillis et al., 2015) and correlates with the thickness of the pillow lava dominated region at the top of each section. This is consistent with the idea that the occurrence of a significant number of sheet flows substantially decreases the bulk crustal permeability (e.g. Bach et al., 2004; Fisher et al., 2014; Gillis et al., 2015). Beneath the well-ventilated zone, calcite formation temperatures increase with depth and the temperature gradient is similar to the conductive geotherm for young oceanic crust (Fig. 2). This increase in paleo-fluid temperature along a conductive geotherm indicates fluid fluxes were much smaller at these depths than in the well-ventilated zone. A change in the conditions of fluid-rock reaction at these depths is also consistent with an observed change in secondary mineral assemblage (Fig. 2).

Simple thermal models allow some quantitative constraints to be placed on the fluid fluxes through the well-ventilated region. The maximum fluid flux is that required to transport all of the heat released by the lithosphere for a given increase in fluid temperature. Between 0 and 20 Myr the average predicted lithospheric heat flux is ~225 mW m^{-2} (e.g. Hasterok, 2013), equivalent to $1.4x10^{14}$ J. For a fluid heat capacity of 4000 J Kg^{-1} K^{-1}, and assuming the average fluid is heated 10°C, this requires a fluid flux of ~$3.5x10^{9}$ kg m^{-2} (or twice as much for a 5°C change in fluid temperature). Alternatively, using the global average hydrothermal heat flux for this age range (Hasterok, 2013) gives ~2 to 4 $x10^{9}$ kg m^{-2} for 5 to 10°C heating of the fluid. These time integrated fluid fluxes are equivalent to water-to-rock mass ratios (i.e. total mass of water passing through a total mass of rock) of ~3,500 to 12,000 assuming an average well-ventilated region 200 m deep and a rock density of 2800 kg m^{-3}; while the absolute values are uncertain the order of magnitude is well constrained.

3.3. Geochemistry

3.3.1. Depth and geological setting dependence of compositional changes

Whole rock compositions provide insight into the chemical exchange between the ocean and lavas during off-axis hydrothermal circulation. For some elements the difference between fresh- and altered-rock compositions are sufficiently large that the protolith composition is not critical and these are considered first. Whole rock CO_2 contents track the amount of calcite added to the lavas as pseudomorphs and in micro-voids, but underestimates the total amount of CO_2 added because calcite also occurs in large voids (see below). Whole rock CO_2 contents generally decrease with depth in all

study areas with significantly thinner CO_2-enriched regions in the Onophrious and Mitsero sections than in the Akaki and Politico sections (Fig. 2). Importantly, substantial CO_2 uptake only occurs in the well-ventilated region of the lavas; i.e. the upper 100-300 m (Fig. 2). In this region there is also a large enrichment in K_2O, and significant depletion in Na_2O. Below the well-ventilated zone samples tend towards protolith-like compositions (Fig. 2). There are no obvious systematic differences in the CO_2, Na_2O or K_2O contents of the cores and rims of lavas (or other elements Fig. S2) at a given depth, except in the Onophrious area where sheet interiors have higher Na_2O than their rims. The lack of strong compositional zoning within individual lava units, alongside large compositional differences between the well-ventilated and underlying poorly-ventilated regions, suggests that large-scale hydrological conditions are critical for controlling exchange of CO_2, Na_2O and K_2O between the ocean and lavas.

In contrast to K_2O and CO_2 (and to a lesser extent Na_2O), the variability in most other major elements in the protolith is of a similar magnitude to that due to alteration. Thus, it is necessary to consider element variability relative to that of potential protoliths which are constrained here using volcanic glass compositions. Volcanic glasses define a tight correlation between CaO and MgO but altered rocks either have protolith-like compositions or have lower CaO_{sil} and/or higher MgO relative to this (Fig. 3a). Olivine accumulation (as phenocrysts) could lead to higher bulk-rock than glass MgO contents but this would only affect primitive (i.e. high MgO) samples; such an effect is not observed indicating that the origin of the elevated MgO/CaO in the altered rocks is largely due to fluid-rock reaction. To compare glass and whole-rock SiO_2 contents we look at changes in the ratio of SiO_2/Al_2O_3 as a function of the sample TiO_2 content under the assumption that Al_2O_3 and TiO_2 are largely immobile during hydrothermal alteration. At any given TiO_2 content, glasses define a limited range of SiO_2/Al_2O_3 but whole rock analyses generally have lower SiO_2/Al_2O_3 suggesting SiO_2 loss during alteration (Fig. 3b). Notably, the similar Al_2O_3/TiO_2 of glasses (9-35; largely decreasing with differentiation) and altered rocks (9-38 excluding one breccia sample) supports the suggestion that these elements are largely immobile (see also Section 3.3.2) and that the glasses span the range of protoliths for the altered rocks.

The whole-rock data (Figures 2 and 3) allow comparison of the compositions of surface samples and drill core samples from the CY1/1A drill core that make up most of the data from the Akaki section. There are no obvious differences that can be put down to either recent weathering affecting the surface samples nor difference in sample availability in a drill core with >90% recovery and surface sampling. This is consistent with the findings of Gillis and Sapp (1997) who showed that surface samples and drill core samples have very similar fracture densities.

In summary, the data demonstrate that hydrothermal alteration led to large (wt% level) changes in the CO_2, Na_2O, MgO, SiO_2, K_2O and CaO of the Troodos lavas (cf. Bednarz and Schmincke, 1989) in all study areas. Similarly large chemical changes are clear in the detailed study of a single outcrop (Section 3.3.2).

3.3.2. Chemical heterogeneity within lava units

Pillows and sheets commonly have interflow material (altered glass ± hydrothermal mineral cement) that, after alteration, can be quite different in composition to the crystalline interior of the lava body. To assess how this chemical heterogeneity affects the bulk changes in crustal composition during alteration, three spatially

contiguous pillows, and their interpillow material, were sampled in detail at the top of the Akaki section within the well-ventilated region (Fig. S1). The compositional variation within these pillows also allows us to determine the impact of where discrete samples are taken within a lava unit (e.g., rim versus core) on measured compositions.

Before determining the chemical changes associated with the pillow outcrop, we further test which elements are immobile during low-temperature alteration because the protolith can safely be assumed to have been very similar for all samples. The ratio of the immobile elements Al_2O_3/TiO_2 in all samples from the three adjacent pillows are between 25.7 and 27.3 (average 26.5±0.4; Fig. 4a). This variability is largely explained by estimates of analytical uncertainty based on replicate analyses (0.05 and 0.01 wt% respectively for Al_2O_3 and TiO_2) suggesting that these "immobile elements" were not redistributed relative to one another. Some interpillow samples are somewhat enriched in Al_2O_3 relative to TiO_2 (Al_2O_3/TiO_2 28.1-30.0) suggesting the addition of high Al_2O_3/TiO_2 phases, most likely clay minerals and/or zeolites, to this zone. Of the other major elements, P_2O_5 and FeO appear to have been relatively immobile in the pillows. As with Al_2O_3, but to a much larger extent, FeO is enriched in interpillow material relative to TiO_2 (by ~15%) indicating significant FeO addition to the interpillow material. Because FeO is not depleted in the pillow interiors this suggests transport of FeO from elsewhere in the crust (possibly associated with observed MnO_2 mineralization). Phosphorous contents are similar to those of glasses with similar immobile element abundances although they are more variable with the relative standard deviation in P_2O_5/TiO_2 of ~40% (25% if two samples are excluded), although this partially reflects imprecision of XRF data at ~0.03 wt% P_2O_5. Overall, these data strongly suggest that TiO_2 and Al_2O_3 are very immobile under the low-temperature, high fluid flux, conditions of alteration experienced by this outcrop and that P_2O_5 is probably the least mobile of the other major elements.

The compositions of the three adjacent pillows are very different to any possible protolith indicating substantial chemical exchange with the aquifer fluid (Fig. 4). The compositional zoning across the two larger pillows (with rims depleted in CaO_{sil}, MgO and Na_2O and enriched in K_2O compared to the core compositions or any likely protolith) indicates incomplete chemical equilibration between the aquifer fluid and rocks. The smallest pillow is compositionally similar to the rims of the larger pillows suggesting its small size allowed a closer approach to complete equilibration. Interpillow material is highly heterogeneous (Fig. 4) and is strongly enriched in CO_2 (averaging 10.8 wt% CO_2 broadly consistent with the report of 29-40 vol% carbonate in the interpillow material; Gillis and Sapp, 1997) compared to the pillows (average 1.6 wt% CO_2). This enrichment of CO_2 in the interpillow material largely reflects the heterogeneous distribution of void space for carbonate to fill. This suggests that sampling of pillow and sheet flows, but not inter-lava material, will underestimate the amount of CO_2 added to the lavas. For example, in this outcrop the 18% interpillow material (Gillis and Sapp, 1997) contains 60% of the CO_2 in the bulk outcrop. This problem, of sampling biases leading to the CO_2 content of the lavas being underestimated, is probably exacerbated in drill cores which average ~30% recovery and preferentially recover the most competent material.

It is important to consider whether our sampling of the core and rim of cooling units allows us to determine a bulk composition of an outcrop and, if so, what fraction of core versus rim analyses should be used to do so. We use the detailed pillow zoning

profiles to test this. To determine the composition of the bulk outcrop we use the pillow sizes and proportions of pillow-versus-interpillow material from Gillis and Sapp (1997; Supplementary Table S4) and the composition data shown in Fig. 4. A linear regression (except for Na were a polynomial was used) through all the whole rock data as a function of distance from the pillow rim was performed allowing the composition of a pillow of any radius to be calculated. These were then used to determine the bulk composition of each pillow measured by Gillis and Sapp (1997) assuming either spherical (maximum amount of rim material) or infinitely long cylindrical (minimum amount of rim material) pillows. These bulk pillow compositions were averaged, weighted by their volume, and mixed with the average interpillow material in the observed proportions (0.82:0.18; Gillis and Sapp, 1997). The bulk outcrop compositions so derived are compared to the measured sample compositions in Fig. 4. Samples collected 10-30 cm from the rim generally provide the best estimate of the bulk outcrop composition. Simple mixing models (Supplementary material S2.3) suggest that a mixture of 30-40% of our typical core sample with 70-60% of our typical rim sample reproduces the bulk outcrop composition best. We consider this below when determining crustal scale compositional changes.

4. CHEMICAL CHANGES DUE TO SEAFLOOR WEATHERING

Section 3 demonstrates that alteration of the Troodos lavas was associated with large changes in the concentration of several major ions (CO_2, Na_2O, MgO, SiO_2, K_2O, CaO; Figs. 2 to 4) while Al_2O_3, TiO_2 and P_2O_5 were largely immobile. This result is consistent with, but expands to a regional scale, previous studies of the CY1/1a drill cores (e.g., Bednarz and Schminke, 1989; Gillis and Robinson, 1990). Notably, the changes in lava composition are largest in the well-ventilated region of the lavas altered at near bottom water temperature (Fig. 2). In this section we determine sample scale chemical changes and then extrapolate these to average changes in the seafloor weathering zone.

4.1. Identifying appropriate protolith compositions

When using altered rock compositions to calculate changes in the composition of the lavas due to hydrothermal alteration, a critical first step is to define a protolith composition to compare to the altered rock. The obvious protolith to use for seafloor lavas is cogenetic volcanic glass that is generally preserved in all but the most pervasively altered ocean crust. However, variations in both parental melt compositions and the extent of igneous differentiation mean that there is not a single protolith composition – indeed fresh glass show a wide range of compositions (e.g. Fig. 3). Our approach to determining the best protolith composition for each whole rock analysis is to select the most representative (see below) glass composition from 137 glass samples (Supplementary Table S2, Regelous et al., 2014) collected from the same geographical area as the whole-rock samples come from (Fig. 1). As a filter on the protoliths we divide them into a more evolved suite and a more primitive suite that are separated based on the abundances of MgO (for glass) and Cr (for glass and whole rocks). Primitive protoliths have MgO > 5.5 wt% and Cr > 15 ppm (n = 71) and evolved protoliths have MgO < 4.75 wt% and Cr < 15 ppm (n = 66).

The concentrations of the least mobile major elements (Al_2O_3, TiO_2 and P_2O_5) are used to identify the most representative protolith for each altered rock. Assuming that there is an appropriate protolith in the glass dataset, for at least one possible protolith the

immobile element abundances in the altered rock should match the protolith abundances multiplied by a constant factor (*c*) that accounts for mass changes (e.g. Grant, 1986). This factor is the ratio of the mass of the original rock to that of the altered rock and accounts for dilution (e.g. by addition of H_2O and CO_2) or concentration (e.g. through Ca- and/or Si-leaching). In other words, a plot of protolith versus altered rock compositions, forced through the origin, gives a straight line with the slope being the factor *c* (e.g. Grant, 1986).

To determine the most likely protolith compositions for each altered rock we performed a linear regression of its Al_2O_3, TiO_2 and P_2O_5 against those of every glass in either the primitive or evolved protolith glass suite depending on the Cr content of the altered rock. Element abundances (*X*) were weighted by their analytical uncertainty based on replicate analyses of volcanic glasses, as this is well quantified and is routinely larger than the uncertainties from whole rock XRF analyses (σ), and the regression was forced through the origin. The best fit protolith is the one with the smallest root mean square difference (RMS_{misfit}) of the mass-change corrected abundance of the immobile elements in the altered rock and the protolith, with each element normalized to its analytical uncertainty:

$$RMS_{misfit} = \sqrt{\left(\frac{1}{n}\right)\sum \frac{\frac{X_{meas}}{c} - X_{glass}}{\sigma_x}} \qquad \text{(Eq. 1)}$$

where *meas* is the measured whole rock composition and *glass* is the measured glass composition and *X*'s are the elements Al_2O_3, TiO_2 and P_2O_5 (hence $n = 3$). The best fitting four protoliths were determined and their standard deviation is used as an estimate of the uncertainty in the protolith composition. For CO_2 the protolith is assumed to be CO_2 free so the measured CO_2 content is the amount added, and the uncertainty is simply the analytical uncertainty.

If a sample contains accumulated crystals (i.e. phenocrysts that did not simply crystallize from their host melt) then this will modify the protolith composition. In the study area, olivine is the only significant phenocryst and is generally rare except in the uppermost lavas. Because the elements used in assigning the protolith are not incorporated in any significant quantity in olivine, protolith selection is unaffected by the presence of olivine (dilution by the presence of phenocrysts is minor and will be accounted for in the dilution factor *c* in Eq. 1). However, if the protolith contained accumulated olivine it would significantly modify the actual protolith composition, especially for MgO. Accumulation of olivine would be expected to lead to a large increase in the Ni content of a sample due to the high partition coefficient for Ni into olivine (~10-15) provided that alteration did not mobilize the Ni. There is little evidence for high Ni/Cr in our whole rock samples. Instead, the range of Ni contents, and the covariation of Ni and Cr (another compatible element, but one that is much less mobile than Ni) suggest that there was little olivine accumulation in almost all samples (Fig. 5). This suggests that olivine accumulation has not substantially modified the whole rock compositions and that much of the olivine observed in the samples crystallized from its host magma; i.e. the whole rock compositions are similar to those of melt.

We performed a series of tests to determine how well our approach to determining the protolith works (Supplementary material S2.1). First, for a small number of samples

we analysed a glassy margin of the same unit that a whole-rock sample came from and compare the glass and calculated protolith compositions (Fig. S3). Second, for a larger number of samples we analysed the rim and interior of a lava unit (sheet or pillow) and compare their protolith compositions, which are expected to be similar (Fig. S3). Likewise, samples collected from core-to-rim through individual pillows are expected to have the same protoliths and the detailed sampling of the Akaki upper pillows (Fig. 4) is used as a test of whether the approach developed above extracts the same protolith (Fig. S4). Finally, the analysis was performed on synthetic data, generated by adding noise to the protolith compositions, to determine how well these could be recovered (Fig. S5). The results show that while there are significant uncertainties in the calculated protolith compositions: (i) there are no systematic offsets between "known" and predicted compositions as shown by the small absolute differences in average compositions (Figs. S3, S4, S5), and (ii) the uncertainty in protolith composition estimated in our approach captures the uncertainty well (compare histograms and probability distributions from modelling in Figs. S3, S4 and S5). Because of the large number of samples used to calculate the overall chemical changes, and the lack of any systematic biases, the average compositional changes determined here are well-constrained.

4.2. Calculated changes in sample compositions

We applied the approach described above to determine the change in composition of samples due to low-temperature, off-axis, hydrothermal alteration in the Troodos ophiolite (Fig. 6). There is significant variability in the extent of compositional change between samples that relates to variation in the extent of alteration, differences in secondary mineralogy, depth in the lavas and uncertainties in the assignment of the protolith. However, robust systematic changes in composition match those expected based on qualitative analysis (Figs. 2 and 3). CaO_{sil} is very strongly depleted (average >5 wt%) in the Troodos lavas, SiO_2 and Na_2O less so, and K_2O is strongly enriched (>2 wt%; Fig. 6). MgO is both depleted in some samples and enriched in others with little change in the bulk lava composition. Samples from the well-ventilated portion of the lava sequence stand out in having substantially larger SiO_2, CaO_{sil} and Na_2O depletions than the average lava and having gained substantially more K_2O (Fig. 6). Only for MgO is there no obvious difference between the changes in composition for samples from the well-ventilated region versus deeper in the lava section. Thus, seafloor weathering in the Troodos ophiolite, under warm bottom water conditions in the late Cretaceous, acted as a source of Ca, Si and Na to the ocean and a sink for K and C. Ages of celadonite, a major sink for K, and calcite demonstrate that these elements were added during seafloor weathering and are not related to uplift (Gallahan and Duncan, 1994; Staudigel et al., 1986).

4.3. Regional scale compositional changes

To determine bulk chemical exchange between the ocean and upper oceanic crust during seafloor weathering (i.e. in the well-ventilated zone; Fig. 2) we need to extrapolate the changes in individual sample compositions to a regional scale. This involves consideration of several characteristics: (i) differences in chemical exchange as a function of depth in the lava sequence (Fig. 2); (ii) differences in chemical exchange as a function of paleo-seafloor topography due to its effect on hydrology; and (iii) compositional zoning within lava units (Fig. 4). Estimates of the regional scale chemical changes

associated with seafloor weathering are made for various assumptions about these factors (see also Supplementary material S2.2).

To account for the significant effect of depth on the extent of alteration within the well-ventilated region (Fig. 2), we determine the average compositional changes in four, equal size, depth intervals from the top to base of the well-ventilated zone. These are combined into two bulk compositional changes; the first weights the study areas by the thickness of their well-ventilated region ("weighted by thickness" model in Table 1) and the second simply averages the bulk changes across the four areas with no weighting ("no weighting" model in Table 1). These alternatives reflect the possibilities that the differences in bulk compositional changes between areas are, or are not, related to differences in the thickness of the well-ventilated region. We also generated estimates of regional bulk composition changes under the assumption that the fraction of different seafloor bathymetries represented by our four study areas is an important control on the bulk chemical changes. To explore the chemical changes in this scenario, we weight the compositional change for each transect by the fraction of that seafloor morphotype in the study area (20% high; 5% low; 75% flat, as determined by mapping) and repeat the averaging described above assuming the thickness of the seafloor weathering zone is independent of the seafloor morphology ("weighted by bathymetry" model in Table 1). Finally, because we sampled pillow rims and interiors in some locations, and pillow rims are more representative of the bulk-outcrop composition (Fig. 4), we determine the difference this makes in the calculated regional compositional changes by using only pillow rims (but all sheet flow analyses) in determining the regional compositional changes ("rim emphasis" model in Table 1); this probably represents an upper limit on the regional compositional changes given that comparison of the composition of a bulk outcrop and individual samples suggest that a mix of 60-70% rim compositions with 30-40% core compositions gives the best estimate of the entire outcrop composition. The end-member is provided here as a limit on the range.

Uncertainties on the regional-scale chemical changes were estimated by bootstrapping (see Supplementary material Section S2.2). The bootstrap samples were then combined, either by depth interval or by study area, weighted appropriately, and then averaged to give the bulk chemical change and the standard deviation of the estimates is given as an estimate of the uncertainty. The four estimates of the average regional scale changes in rock composition due to seafloor weathering in the Troodos ophiolite are within uncertainty of one another (Table 1). These estimates are also generally similar to those of Bednarz and Schminke (1989) determined in an entirely different way using samples just from the CY1 drill core. Thus, the compositional changes due to seafloor weathering determine here (Table 1) are considered robust.

5. THE EFFECT OF BOTTOM WATER TEMPERATURE ON CHEMICAL CHANGES DURING SEAFLOOR WEATHERING: COMPARISON TO DSDP-ODP DRILL CORES

To be able to examine the role of changing bottom water temperature on the chemical fluxes associated with off-axis hydrothermal systems we would ideally use similar datasets to that presented here for the Troodos ophiolite, but for crust altered under different bottom water temperatures. Unfortunately, the Troodos ophiolite is the only ophiolite that we are aware of that contains a record of low-temperature alteration

that has neither been significantly overprinted during obduction, nor was anomalous in having very high initial sedimentation rates. This leaves us reliant on drill cores from the modern ocean basins for which it is difficult to assess the representativeness of the sampling considering cores are ~6 cm wide and generally recovery is <50% (e.g. Supplementary Table S5). Review of drill cores through the lava section of the oceanic crust shows that only six fulfill the following criteria: (i) altered under well-ventilated conditions as determined by carbonate O-isotope temperatures that do not vary systematically with depth and are similar to contemporaneous seawater, and (ii) sufficient whole-rock and glass data (compiled from PetDB) to calculate meaningful changes in lava composition (Supplementary material S3 and Fig. S6). See Supplementary Table 5 for a summary of the characteristics of the selected sites.

To calculate sample scale chemical changes for the drill cores we used the same approach as for the Troodos ophiolite except: (i) the general lack of Cr data precluded using Cr as a filter on potential protoliths, and (ii) the common existence of plagioclase in these cores means we have to consider mixtures of glass and plagioclase as potential protoliths. To achieve this we mathematically mixed the average reported plagioclase composition (An_{62} to An_{75}; Supplementary material S3) with each glass composition in different proportions to generate a suite of potential protoliths. The bulk compositional change for each drill core was determined from the average of all samples and the standard deviation on this is used as an estimate of the uncertainty (Table 1). Unfortunately given core recovery averaging <50%, and the limitations imposed by availability of information about these cores, more detailed analysis of the uncertainties is not warranted.

Previous studies of chemical changes associated with off-axis hydrothermal alteration have not focused on the well-ventilated region and have used a range of different approaches to determining compositional changes making comparison of the results of this study and previous work largely meaningless. Comparing bulk chemical changes from drill cores that were not altered under well-ventilated conditions with those that were is beyond the scope of this study of seafloor weathering. For the well-ventilated sites studied here, only DSDP Hole 417A has a previously published estimate of the chemical fluxes associated with off-axis alteration (Staudigel et al., 1989; 1996). This was drilling on a topographic high that was open to seawater circulation for > 30 m.y. and that is extensively altered, for example having a high K content (Alt and Honnorez, 1984; Staudigel et al., 1996). In this Hole the upper, pillow- and hyaloclastite dominated, portion of the core shows much larger effects of low-temperature alteration than the lower half where massive flows are more common (Alt and Honnorez, 1984) consistent with the observation in the Troodos ophiolite (Fig. 2). The adjacent Holes 417D and 418A show lesser chemical changes most likely due to being drilled on flat seafloor that was sedimented much earlier. These cores contain carbonates formed at temperatures inconsistent with well-ventilated conditions, thus they are not considered further here. Staudigel et al., (1996) used a very different approach to determining the chemical changes in Hole 417A than used here. Their results suggest massive Al mobility (including a gain of 3.5 wt% Al_2O_3 overall) something we see no evidence for and interpret as being a result of a problem with their methodology. Thus we do not undertake a detailed comparison of the results of this and other studies. Dredged samples offer another potential suite to investigate seafloor weathering however they are difficult to

treated quantitatively because of the general lack of glass to provide protolith compositions. Additionally, they generally only come from young crust as older crust is largely sediment covered. However, small changes in bulk K contents have been reported for dredge suites collected on late Cenozoic crust and larger ones for suites from Cretaceous crust (e.g. Schram et al., 2005; Hart 1970; Mathews, 1971) – whether this is meaningful is unclear but the data are at least consistent with those from drill cores and Troodos ophiolite.

The only drill core with compositional changes of a similar magnitude to those in the Troodos ophiolite is the 120 Myr old Site 417A, which was also altered under warm bottom water conditions. In contrast, those sites that were altered under cooler bottom water conditions show much smaller chemical changes (Table 1). The magnitude of SiO_2, Na_2O and CaO depletion, and K_2O and CO_2 enrichment, increase with increasing average temperature of calcite precipitation (Fig. 7). There is, however, substantial scatter in the data and hence substantial uncertainty on the exact temperature dependence of the extent of chemical exchange during seafloor weathering. This is unsurprising given that local hydrological conditions will be critical in controlling the chemical fluxes and incomplete recovery probably biases drill core bulk compositions. Linear fits through the compositional changes as a function of alteration temperature are shown in Fig. 7 and given in Table 2. These are forced through the origin for Si, Mg, K and C (i.e. always into or out of the ocean) because it is unlikely that the sign of the flux changes for these elements. For Ca and Na changes in sign are possible (e.g. Wheat et al., 2017) and the regressions for these elements are not forced through the origin. Linear fits are used simply because the data do not justify anything else and should not be taken to imply the true changes will be linear. The behaviour of MgO is more complex with either release from the crust or uptake into the crust plausible given these data. The reason for this is discussed in Section 6.2.

A somewhat independent test of the role of bottom water temperature in determining the extent of major ion exchange between the ocean and lavas in off-axis hydrothermal systems comes from previously reported bulk core CO_2 contents (Fig. 7f; Staudigel et al., 1989; Alt and Teagle, 1999; Alt, 2004; Gillis and Coogan, 2011). Unlike the whole-rock data considered here, these include visual estimates of void filling (e.g. vein, breccia) carbonate as well as the pervasively distributed carbonate that is quantified through whole-rock analysis. Because formation of carbonate minerals generally requires extensive fluid-rock reaction to generate the alkalinity needed for sustained calcite saturation (Coogan and Gillis, 2013) bulk-CO_2 is a proxy for the 'extent' of low-temperature fluid-rock reaction. Holes are excluded if their average carbonate formation temperature is >10°C above contemporaneous bottom water temperature as this would generally indicate restricted fluid flow (unless there was a very thick sediment pile). This larger and more robust dataset shows a similar correlation of CO_2 uptake and carbonate precipitation temperature to that for the well-ventilated sites studied here but with greater CO_2 uptake (due to the inclusion of void-filling carbonate). This observation supports the hypothesis that bottom water temperature is a prime control on the extent of chemical exchange in off-axis hydrothermal systems.

It is important to note that alteration at high temperatures due to restricted fluid flow (e.g. due to high sedimentation rates or sheet flows reducing the bulk permeability) will not have the same effect as alteration under conditions of high bottom water

temperature. In the former case restricted fluid flow will lead to large changes in the fluid composition but the small fluid fluxes will lead to small total chemical fluxes and limited rock alteration (e.g. Bach et al., 2004). A good example of this situation, that is not considered further here, is the Juan de Fuca plate where a thick sediment blanket on young crust leads to a high aquifer temperature (~63°C) with a very evolved fluid composition (e.g. almost no Mg) but very small fluid fluxes (Wheat and Mottl, 2000; Winslow et al., 2016).

6. SEAFLOOR WEATHERING: CONTROLS AND CONSEQUENCES

In this section we discuss three topics. First, the origin of the temperature dependence of chemical exchange between the ocean and crust during seafloor weathering is considered. Second, we discuss changes in the aquifer fluid composition and how these affect mineral stability and in-turn lead to mineral precipitation in void spaces in the crust. Finally, we give an example of how changing bottom water temperature could drive changes in the chemical fluxes between the ocean and upper oceanic crust due to seafloor weathering.

6.1. Controls on seafloor weathering

The principle controls on the chemical fluxes associated with off-axis hydrothermal systems are the temperature of fluid-rock reaction, fluid flux, and composition of contemporaneous seawater. We have investigated the portion of these systems where alteration occurs at near bottom-water temperature (Fig. 2, Fig. S6) due to large fluid fluxes. Comparison of the chemical changes determined for the Troodos ophiolite with data from drill cores from the modern ocean basins is consistent with the hypothesis that bottom water temperature plays an important role in controlling the magnitude of chemical exchange (Fig. 7). The empirical data used here does not allow the relative roles of changing thermodynamics and kinetics with changing fluid temperature to be unraveled. An important role for kinetics is suggested by: (i) the compositional zoning across pillows from a single outcrop (Fig. 4) which indicates incomplete equilibration during alteration as has been widely documented (e.g. Böhlke et al., 1981); (ii) the much greater extent of mineralogical recrystallization in the Troodos ophiolite and DSDP Hole 417A than in the sites altered at cooler conditions (e.g. Honnorez et al., 1978; Alt and Honnorez, 1984; Gillis and Robinson, 1990; Paul et al., 2006); and (iii) the Sr-isotopic composition of carbonates from the upper oceanic crust that show strong evidence for the importance of temperature in controlling the rate of rock dissolution (e.g. Coogan and Dosso, 2015). Thermodynamic constraints on mineral stability (both degree of under saturation of primary phases and over saturation of secondary minerals) must also play some role but the importance of this requires further investigation.

The fluid flux and the composition of contemporaneous seawater are also expected to affect chemical fluxes in off-axis hydrothermal systems. The role of fluid flux is minimized in the analysis presented above by investigating only well ventilated regions where fluid fluxes were sufficiently large to maintain near bottom water temperatures. The composition of seawater however cannot be isolated from its temperature using available empirical data because the temperature and composition of bottom water have both changed over the last 120 Myr. The large changes in the uptake of CO_2 into the crust, that largely depend on the extent of alkalinity generating fluid-rock

reaction and are only weakly influenced by the composition of seawater (Coogan and Gillis, 2013), suggest that temperature changes play a key role. Thus, we suggest that global chemical fluxes from off-axis hydrothermal systems appear to be sensitive to changes in bottom water temperature. Of course, in any given location hydrological conditions can dominate, and testing this hypothesis will require comparing regions with similar paleo-hydrology.

6.2. Evolution of the aquifer fluid

Small relative changes in the major ion abundances in the main aquifer fluid are predicted to occur during seafloor weathering despite large changes in the rock composition due to the large water-to-rock ratios. For example, assuming a reasonable water-to-rock ratio of 2000, leaching 3 wt% CaO from the rock, and adding 3 wt% K_2O to the rock, would change the hydrothermal fluid Ca and K contents by <0.5 mmol kg^{-1} (i.e. <5%). Such changes would not substantially change mineral stability; i.e. phases precipitated from the main aquifer fluid must be close to saturation in seawater. Only in local geochemical environments, such as micropores containing stagnant fluid, where the fluid composition can evolve to much more extreme compositions, would other phases be precipitated (e.g. as pseudomorphs).

In contrast to most major ions such as Mg, Ca and K, relatively large changes in the main aquifer fluid are predicted to occur for: (i) Si; (ii) the carbon system (pH, alkalinity, CO_2 etc); and (iii) some oxidants in the fluid (O_2, NO_3^-). Thus, it is these species that are likely to control secondary mineral precipitation in major void spaces. Large relative changes of fluid SiO_2 contents may be critical in changing silicate mineral stability. For example, leaching 3 wt% SiO_2 at a water-to-rock ratio of 2000 would lead to an increase in fluid Si content of 0.25 mmol kg^{-1} (compared to an average modern seawater Si of ~0.1 mmol). Increased fluid Si will tend to favour K-feldspar formation over clay minerals and K-micas (MacKenzie and Garrels, 1966; Garrels, 1984). This may explain the common occurrence of K-feldspar in Cretaceous but not late Cenozoic altered upper oceanic crust (Coogan and Gillis, 2013) due to the higher temperature alteration of the former leading to more Si being leaching from the rock.

Leaching of Si can also potentially explain the observed large-scale precipitation of Mg-silicates in voids (e.g. smectite in veins and breccia cements) and the generally enigmatic behaviour of Mg in off-axis hydrothermal systems. Sediment pore fluid data (e.g. Mottl and Wheat, 1994) and experimental data (e.g. Seyfried and Bischoff, 1979) indicate Mg is generally added to the crust with increasing fluid temperature. However, there is extensive evidence that under some conditions, especially right at the seafloor (e.g. dredge samples), Mg can be lost from the crust (Hart, 1970; Mathews, 1971; Honnorez, 1981; Fig. 4). Substantial Mg-loss has also been documented in the uppermost portion of DSDP Site 417A (Staudigel et al., 1996; Alt and Honnorez, 1984). Alteration under low pH and low Mg conditions inhibits formation of Mg-clays (Harder, 1972; Drever, 1974) and this has been suggested as a possible cause for Mg loss from lavas (Seyfried et al., 1978), but this is unlikely to be the case for near-seafloor samples. Instead, samples at or very near the seafloor may be altered under conditions of sufficiently high water-to-rock ratio that the fluid Si content does not become sufficiently elevated (or conditions where diffusive Si exchange with the ocean maintains low fluid Si content) to stabilize Mg-silicates. Deeper in the crust, where higher fluid Si contents would be expected, Mg-silicate precipitation could occur driven by increased $a(SiO_2)_{aq}$,

and the bulk crust Mg content would increase (and fluid Mg content decrease). Thus, large-scale Si addition to the fluid (Fig. 7) is probably not associated with an equal magnitude of Si flux to the ocean. Instead Mg-silicate formation probably leads to some of the Si added to the fluid being returned to the rock with seawater-derived Mg, leading to an overall uptake of Mg into the rock. The extent of this is likely to depend on the Mg content of seawater at the time.

In the carbon system alkalinity generation by leaching of cations from the rock will drive the fluid towards $CaCO_3$ saturation (Coogan and Gillis, 2013). As with Mg-silicates, this can lead to $CaCO_3$ precipitation in void spaces modifying the aquifer fluid and bulk-lava compositions. Consumption of the oxidants O_2 and NO_3^- by (possibly microbial mediated) fluid-rock reactions is predicted to lead to large-scale depletion of these species in the aquifer fluid (Bach and Edwards, 2003; Stolper and Keller, 2018). In turn, this will change the mobility of redox sensitive elements. This may explain the behaviour of Mn and Fe, which can be mobilized in areas of the crust in which the aquifer fluid is relatively reduced and re-precipitated where the fluids becomes more oxidized (e.g. closer to the seafloor). For example, the inter-pillow material in the near-seafloor outcrop studied in detail (Fig. 4) is enriched in both Mn and Fe.

6.3. Changes in seafloor weathering fluxes with bottom water temperature

The temperature dependence of chemical exchange during seafloor weathering (Table 2) allows prediction of how chemical fluxes associated with off-axis hydrothermal systems will respond to changing bottom water temperature. An example of this for the last 100 Myr is shown in Fig. 8. Bottom water temperature is taken from Cramer et al. (2011) and ranges from 0 to 18°C and the aquifer fluid is assumed to be 5°C warmer than this. The mass of crust that undergoes seafloor weathering is held constant to elucidate the role of bottom water temperature in controlling the fluxes. This assumption is equivalent to assuming: (i) the average crustal production rate stays constant (for consideration of changing production rate, which will have a linear knock-on to the fluxes calculated here, see Müller and Dutkiewicz, 2018), (ii) the average sedimentation rate stays constant, and (iii) the average lithological make-up of the crust stays constant. For the latter point we note that currently the evidence is ambiguous as to whether the fraction of the upper crust comprised of pillows versus sheets changes with spreading rate (e.g. Karson, 2002; Perfit and Chadwick, 1998). There are significant uncertainties in the input for these calculations, both from the thickness of the seafloor weathering zone and the slopes (and linearity) of the calibrations in Table 2, and hence we do not suggest that the exact values of the fluxes are correct. However, two points appear robust. First, the magnitude of the off-axis hydrothermal fluxes due to seafloor weathering are sensitive to bottom water temperature and hence global climate. Second, the magnitude of the off-axis hydrothermal fluxes due to seafloor weathering are generally significantly larger than the axial (black smoker) flux for Ca, Si and K.

7. SUMMARY AND CONCLUSIONS

A detailed study of the exchange of major ions between the ocean and upper oceanic crust due to seafloor weathering in the Troodos ophiolite was undertaken. Transects through four areas in the lavas with contrasting lithological make-up and paleo-topography identified an upper zone with large chemical changes and consistently low alteration temperatures that indicate well-ventilated conditions. The change in

composition of samples from this zone was determined using volcanic glass to define potential protoliths. Various approaches to extrapolate to bulk-upper crustal compositions were considered. The results are compared with changes in the composition of crust recovered by drilling in the modern ocean basins where alteration also occurred under well-ventilated conditions but at different bottom water temperatures. The key results are:

1. A portion of the lavas that make up the upper oceanic crust are generally altered at near bottom water temperature (Fig. 2), a process that can be thought of as seafloor weathering by analogy with continental weathering. The thickness of the seafloor weathering zone appears to depend on the permeability distribution in the lavas (pillows versus sheets) but the extent of chemical exchange must also be affected by the regional sedimentation rate. Chemical exchange during alteration in this well-ventilated zone is strongly dependent on bottom water temperature (and hence global climate; Fig. 7).
2. The major ion content of the main aquifer fluid changes little during seafloor weathering due to high water-to-rock ratios. Changes in the fluid Si, C-system, and oxidants (O_2, NO_3^-) are probably responsible for driving secondary mineral precipitation from the main aquifer fluid (e.g. in inter-pillow zones and other high porosity zones).
3. Preliminary parameterizations for the chemical fluxes due to seafloor weathering, and their dependence on bottom water temperature (and hence climate), are presented (Table 2). However we caution that these are probably modified by secondary mineral precipitation in void spaces within the crust (e.g. loss of Ca and Si due to precipitation of calcite and smectite, respectively). Rough estimates suggest that for many major ions these fluxes are both large relative to the on-axis flux and, more importantly, vary substantially with changing bottom water temperature (Fig. 8).

ACKNOWLEDGEMENTS

The Geological Survey of Cyprus is thanked for support for both the core and field studies. Jody Spence (ICP-MS analyses), Janet Gabites (carbonate O-isotope analyses), Mao Mao, Aerona Moore and Matt Pope (sample preparation) are also thanked for assistance. Geoff Wheat, two anonymous reviewers, and AE Jeff Alt are thanked for comments that improved the manuscript. LAC and KMG were funded through NSERC Discovery (5098 & 155396) and Accelerator grants. The manuscript was prepared while the authors were guests at the Institute of Marine Sciences in Barcelona.

REFERENCES

Alt, J.C., 2004. Alteration of the upper oceanic crust: mineralogy, chemistry, and process, in: Davis, E.E., Elderfield, H. (Eds.), Hydrology of the Ocean Lithosphere. Cambridge University Press, Cambridge, pp. 495–533.

Alt J. C. and Honnorez J. (1984) Alteration of the upper oceanic crust, DSDP Site 417: mineralogy and chemistry. *Contrib. Mineral. Pet.* **87**, 149–169.

Alt J. C. and Teagle D. A. H. (1999) The uptake of carbon during alteration of ocean crust. *Geochim. Cosmochim. Acta* **63**, 1527–1535.

Anderson B. W., Coogan L. A. and Gillis K. M. (2012) The role of outcrop-to-outcrop fluid flow in off-axis oceanic hydrothermal systems under abyssal sedimentation conditions. *J. Geophys. Res.* **117**, doi:10.1029/2011JB009052.

Bach W. and Edwards K. J. (2003) Iron and sulfide oxidation within the basaltic ocean crust: implications for chemolithoautotrphic microbial biomass production. *Geochim. Cosmochim. Acta* **67**, 3871–3887.

Bach W., Humphris S. E. and Fisher A. T. (2004) Fluid flow and fluid-rock interaction within ocean crust: Reconciling geochemical, geological, and geophysical observations. In *Subseafloor biosphere at mid-ocean ridges* (ed. Wilcock, WSD, DeLong, EF, Kelley, DS and Baross, JA. AGU Geophysical Monograph Series. pp. 99–117.

Bear L. M. (1960) *Cyprus Geological Survey Department Memoir 3. The geology and mineral resources of the Akaki-Lythrodondha area*, Government of Cyprus, Nicosia, Cyprus, pp 122.

Bednarz U. and Schmincke H.-U. (1989) Mass transfer during sub-seafloor alteration of the upper Troodos crust (Cyprus). *Contrib. Mineral. Petrol.* **102**, 93–101.

Booij E., Gallahan W. E. and Staudigel H. (1995) Ion-exchange experiments and Rb/Sr dating on celadonites from the Troodos ophiolite, Cyprus. Chem. Geol. 126, 155–167.

Böhlke J. K., Honnorez J., Honnorez-Guerstein B.-M., Muehlenbachs K. and Petersen N. (1981) Heterogeneous alteration of the upper oceanic crust: Correlation of rock chemistry, magnetic properties, and O isotope ratios with alteration patterns in basalts from site 396B, DSDP. J. Geophys. Res. Solid Earth 86, 7935–7950.

Brady P. V and Gislason S. R. (1997) Seafloor weathering controls on atmospheric CO_2 and global climate. *Geochim. Cosmochim. Acta* **61**, 965–973.

Coogan L. A., Gillis K. M., Pope M. and Spence J. (2017) The role of low-temperature (off-axis) alteration of the oceanic crust in the global Li-cycle: Insights from the Troodos ophiolite. *Geochim. Cosmochim. Acta* **203**, 201–215.

Coogan L. A. and Dosso S. (2012) An internally consistent, probabilistic, determination of ridge-axis hydrothermal fluxes from basalt-hosted systems. *Earth Planet. Sci. Lett.* **323**, 92–101.

Coogan L. A. and Dosso S. E. (2015) Alteration of ocean crust provides a strong temperature dependent feedback on the geological carbon cycle and is a primary driver of the Sr-isotopic composition of seawater. *Earth Planet. Sci. Lett.* **415**, 38–46.

Coogan L. A. and Gillis K. M. (2018) Low-Temperature Alteration of the Seafloor: Impacts on Ocean Chemistry. *Annu. Rev. Earth Planet. Sci.* **46**, 1-25.

Coogan L. A. and Gillis K. M. (2013) Evidence that low-temperature oceanic hydrothermal systems play an important role in the silicate-carbonate weathering cycle and long-term climate regulation. *Geochem. Geophys. Geosys.* **14**, 1771–1786.

Coplen T. B. (2007) Calibration of the calcite-water oxygen isotope thermometer at Devils Hole, Nevada, a natural laboratory. *Geochim. Cosmochim. Acta* **71**, 3948–3957.

Cramer B. S., Miller K. G., Barrett P. J. and Wright J. D. (2011) Late Cretaceous–Neogene trends in deep ocean temperature and continental ice volume: Reconciling records of benthic foraminiferal geochemistry ($\delta^{18}O$ and Mg/Ca) with sea level history. *J. Geophys. Res. Ocean.* **116**, doi.org/10.1029/2011JC007255.

Demicco R. V, Lowenstein T. K., Hardie L. A. and Spencer R. J. (2005) Model of seawater composition for the Phanerozoic. *Geology* **33**, 877–880.

Drever J. I. (1974) The magnesium problem. In *The Sea* (ed. E. D. Goldberg). Wiley Interscience, New York. pp. 337–357.

Fisher A. T. and Becker K. (2000) Channelized fluid flow in oceanic crust reconciles heat-flow and permeability data. *Nature* **403**, 71–74.

Fisher, A.T., Alt, J.C., Bach, W., 2014. Hydrogeologic Properties, Processes, and Alteration in the Igneous Ocean Crust, in: Developments in Marine Geology, Volume 7. pp. 507–551.

Follows, E.J., Robertson A.H.F., 1990. Sedimentology and structural setting of Miocene reefal limestones in Cyprus, in: Malpas, J., Moores, E.M., Panayiotou, A., Xenophontos, C. (Eds.), Ophiolites: Oceanic Crust Analogues, Proceeding of the Symposium "Troodos 1987." Geological Survey Department, Nicosia, 207-215.

Friedrich O., Norris R. D. and Erbacher J. (2012) Evolution of middle to Late Cretaceous oceans — A 55 m.y. record of Earth's temperature and carbon cycle. *Geol.* **40**, 107–110.

Gallahan W. E. and Duncan R. A. (1994) Spatial and temporal variability in crystallization of celadonites within the Troodos ophiolite, Cyprus: Implications for low-temperature alteration of the oceanic crust. J. Geophys. Res. Solid Earth 99, 3147–3161.

Garrels R. M. (1984) Montmorillonite/illite stability diagrams. *Clays Clay Miner.* **32**, 161–166.

Gibson I. L., Malpas J., Robinson P. T. and Xenophontos C. (1991) *Cyprus crustal study project: initial report, Hole CY-1 and 1a*. Geological Survey of Canada, 283 pp.

Gillis K. M. and Coogan L. A. (2011) Secular variation in carbon uptake into the ocean crust. *Earth Planet. Sci. Lett.* **302**, 385–392.

Gillis K. M., Coogan L. A. and Brant C. (2015) The role of sedimentation history and lithology on fluid flow and reactions in off-axis hydrothermal systems: A perspective from the Troodos ophiolite. *Chem. Geol.* **414**, 84–94.

Gillis K. M. and Robinson P. T. (1988) Distribution of alteration zones in the upper oceanic crust. *Geology* **16**, 262–266.

Gillis K. M. and Robinson P. T. (1990) Patterns and processes of alteration in the lavas and dykes of the Troodos Ophiolite, Cyprus. *J. Geophys. Res.* **95**, 21,521-21,548.

Gillis K. M. and Sapp K. (1997) Distribution of porosity in a section of upper oceanic crust exposed in the Troodos Ophiolite. *J. Geophys. Res.* **102**, 10,133–10,149.

Gillis K. M. and Robinson P. T. (1985) Low-temperature alteration of the extrusive sequence, Troodos Ophiolite, Cyprus. *Can. Mineral.* **23**, 431–441.

Grant J. A. (1986) The Isocon Diagram - a Simple Solution to Gresens Equation for Metasomatic Alteration. *Econ. Geol.* **81**, 1976–1982.

Harder H. (1972) The role of magnesium in the formation of smectite minerals. *Chem. Geol.* **10**, 31–39.

Hart R. (1970) Chemical exchange between seawater and deep ocean basalts. *Earth Planet. Sci. Lett.* **9**, 269–279.

Hasterok D. (2013) Global patterns and vigor of ventilated hydrothermal circulation through young seafloor. *Earth Planet. Sci. Lett.* **380**, 12–20. .

Honnorez J. (1981) The aging of the oceanic crust at low temperature. In *The Sea: Volume 7: The oceanic lithosphere* John Wiley & Sons, New York. pp. 525–587.

Honnorez J., J.L. Bohlke A. and Honnorez-Guerstein B. M. (1978) Petrographical and Geochemical Study of the Low Temperature Submarine Alteration of Basalt from Hole 396B, Leg 46. In *Initial Reports of the Deep Sea Drilling Project, Vol 46* Washington (U.S. Government Printing Office), pp. 299–329.

Karson J. A. (2002) Geologic Structure of the Uppermost Oceanic Crust Created at Fast- to Intermediate-Rate Spreading Centers. *Annu. Rev. Earth Planet. Sci.* **30**, 347–384.

Kim S.-T. and O'Neil J. R. (1997) Equilibrium and nonequilibrium oxygen isotope effects in synthetic carbonates. *Geochim. Cosmochim. Acta* **61**, 3461–3475.

Krissansen-Totton J. and Catling D. C. (2017) Constraining climate sensitivity and continental versus seafloor weathering using an inverse geological carbon cycle model. *Nat. Commun.* **8**, 15423.

Li C. and Ripley E. M. (2010) The relative effects of composition and temperature on olivine-liquid Ni partitioning: Statistical deconvolution and implications for petrologic modeling. Chem. Geol. 275, 99–104.

MacKenzie F. T. and Garrels R. M. (1966) Chemical mass balance between rivers and oceans. *Am. J. Sci.* **264**, 507.

Mathews D. H. (1971) Weathered nnd Metamorphosed Basalts. Altered basalts from Swallow Bank, an abyssal hill in the NE Atlantic, and from a nearby seamount. *Philos. Trans. R. Soc. London A Math. Phys. Eng. Sci.* **268**, 551–571.

Mottl M. J. and Wheat C. G. (1994) Hydrothermal Circulation through Mid-ocean Ridge Flanks - Fluxes of Heat and Magnesium. *Geochim. Cosmochim. Acta* **58**, 2225–2237.

Mukasa S. B. and Ludden J. N. (1987) Uranium-lead isotopic ages of plagiogranites from the Troodos ophiolite, Cyprus, and their tectonic significance. *Geology* **15**, 825–828.

Müller R. D. and Dutkiewicz A. (2018) Oceanic crustal carbon cycle drives 26-million-year atmospheric carbon dioxide periodicities. *Sci. Adv.* **4**, DOI: 10.1126/sciadv.aaq0500.

Paul H. J., Gillis K. M., Coggon, R.M. and Teagle D.A.H. (2006) ODP Site 1224: A missing link in the investigation of seafloor weathering. *Geochem. Geophys. Geosys.* **7**, doi:10.1029/2005GC001089.

Perfit M. R. and Chadwick J. W. W. (1998) Magmatism at mid-ocean ridges: constraints from volcanological and geochemical investigations. In *Faulting and Magmatism at Mid-Ocean Ridges* (eds. W. R. Buck, P. T. Delaney, J. A. Karson, and Y. Lagrabrielle). American Geophysical Union. pp. 59–115.

Porter, S.M., (2010) Calcite and aragonite seas and the de novo acquisition of carbonate skeletons. Geobiology 8, 256–277.

Regelous M., Haase K. M., Freund S., Keith M., Weinzierl C. G., Beier C., Brandl P. A., Endres T. and Schmidt H. (2014) Formation of the Troodos Ophiolite at a triple junction: Evidence from trace elements in volcanic glass. *Chem. Geol.* **386**, 66–79.

Schramm, B., Devey, C.W., Gillis, K.M., Lackschewitz, K., 2005. Quantitative assessment of chemical and mineralogical changes due to progressive low-temperature alteration of East Pacific Rise basalts from 0 to 9 Ma. Chem. Geol. 218, 281–313.

Seyfried W. E. and Bischoff J. L. (1979) Low-Temperature Basalt Alteration by Seawater: Experimental-Study at 70°C and 150°C. *Geochim. Cosmochim. Acta* **43**, 1937–1947.

Seyfried W. E., Shanks W. C. and Dibble W. E. (1978) Clay mineral formation in DSDP Leg 34 basalt. *Earth Planet. Sci. Lett.* **41**, 265–276.

Spencer, R.J., Hardie, L.A., 1990. Control of seawater composition by mixing of river waters and mid-ocean ridge hydrothermal brines, in: Spencer, R.J., Chou, I.M. (Eds.), Fluid-Mineral Interactions: A Tribute to H. P. Eugster. Geochemical Society Special Publication, pp. 409–419.

Sundquist, E.T., 1991. Steady-State and Non-Steady-State Carbonate Silicate Controls on Atmospheric CO_2. Quat. Sci. Rev. 10, 283–296.

Staudigel H., Hart S. R., Schmincke H.-U. and Smith B. M. (1989) Cretaceous ocean crust at DSDP Sites 417 and 418: Carbon uptake from weathering versus loss by magmatic outgassing. *Geochim. Cosmochim. Acta* **53**, 3091–3094.

Staudigel H., Plank T., White B. and Schimincke H.-U. (1996) Geochemical fluxes during seafloor alteration of the basaltic upper oceanic crust: DSDP Sites 417 and 418. In *Subduction: Top to bottom* American Geophysical Union, Washington, DC. pp. 19–38.

Staudigel, H., Gillis, K., Duncan, R., 1986. K/Ar and Rb/Sr ages of celadonites from the Troodos ophiolite, Cyprus. Geology 14, 72–75.

Stein C. A. and Stein S. (1992) A model for the global variation in oceanic depth and heat flow with lithospheric age. *Nature* **359**, 123–137.

Stolper D. A. and Keller C. B. (2018) A record of deep-ocean dissolved O_2 from the oxidation state of iron in submarine basalts. *Nature* **553**, 323.

Wheat C. G. and Mottl M. J. (2000) Composition of pore and spring waters from Baby bare: global implications of geochemical fluxes from a ridge flank hydrothermal system. *Geochim. Cosmochim. Acta* **64**, 629–642.

Wheat, C.G., Fisher, A.T., McManus, J., Hulme, S.M., Orcutt, B.N., 2017. Cool seafloor hydrothermal springs reveal global geochemical fluxes. Earth Planet. Sci. Lett. 476, 179–188.

Winslow D. M., Fisher A. T., Stauffer P. H., Gable C. W. and Zyvoloski G. A. (2016) Three-dimensional modeling of outcrop-to-outcrop hydrothermal circulation on the eastern flank of the Juan de Fuca Ridge. *J. Geophys. Res. Solid Earth* **121**, 1365–1382.

Tables

Table 1 Bulk changes in crustal composition (wt%) in the seafloor weathering zone

Crustal section (age)	T (°C)	SiO_2	MgO	$^{f}CaO_{sil}$	Na_2O	K_2O	CO_2
Troodos ophiolite (91.6 Myr)							
No weighting[a]	16	-3.8 (1.2)	0.7 (0.8)	-7.9 (1.2)	-0.6 (0.4)	3.4 (0.9)	2.5 (1.2)
Weighted by thickness[b]	16	-3.4 (1.3)	0.6 (0.5)	-8.2 (0.8)	-0.6 (0.3)	3.7 (0.9)	2.7 (1.0)
Weighted by bathymetry[c]	16	-3.2 (1.0)	0.6 (0.6)	-8.3 (0.7)	-0.7 (0.3)	3.9 (0.8)	2.7 (0.9)
Rim emphasis[d]	16	-4.2 (1.4)	1.0 (0.8)	-8.4 (0.9)	-0.4 (0.3)	3.5 (0.8)	2.6 (1.2)
DSDP/ODP holes							
396B (13.6 Myr; upper 160 m[h])	1.7	-0.6 (2.1)	-0.1 (0.9)	0.0 (0.6)	-0.2 (0.2)	0.1 (0.1)	0.2 (0.1)
335 (15 Myr)	4.5	-0.2 (1.6)	0.0 (0.7)	-0.6 (1.1)	0.1 (0.2)	0.1 (0.1)	0.4 (0.8)
562 (17.1 Myr)	5.8	0.0 (1.3)	-0.2 (0.5)	0.2 (0.6)	-0.1 (0.2)	0.1 (0.1)	0.3 (0.4)
556 (30.6 Myr)[g]	7.8	0.6 (2.2)	0.7 (1.0)	0.0 (0.8)	0.0 (0.2)	0.1 (0.1)	0.3 (0.5)
1224F (46 Myr)	6.6	2.5 (2.1)	1.2 (0.7)	0.3 (0.5)	-0.1 (0.2)	0.2 (0.1)	0.2[e]
417A (120 Myr)	21.5	-5.3 (2.5)	-1.7 (1.2)	-2.2 (2.9)	-0.3 (0.4)	0.9 (1.3)	0.9 (0.6)

Uncertainties, given in parentheses, are one standard deviation of bootstrapped synthetic datasets for the Troodos ophiolite and the standard deviation of the compositional change derived from the different samples for the DSDP/ODP cores. Temperatures are the mean O-isotope derived carbonate precipitations temperature.

a – unweighted meaning the different crustal sections have equal influence on the bulk compositional change calculated.

b – weighted by the thickness of the well-ventilated region in each crustal section. Hence the deeper sections (Akaki and Politico) are weighted more heavily than the shallower sections (Mitsero and Onophrious).

c – weighted by the proportion of the study area (Fig. 1) that has the seafloor morphology of each area.

d – excluding pillow interiors and weighted by the thickness of the well-ventilated region.

e – From Paul et al. (2006)

f – The carbonate correction for CaO_{sil} is less well constrained for the DSDP/ODP samples than Troodos ophiolite because CO_2 data is not available for all samples. However, the corrections for carbonate content are generally small and thus introduce second-order uncertainties.

g – lavas overlie a gabbroic breccia

h – this limits the samples used to those in the region of the core with carbonate O-isotope thermometry.

Table 2 Parameterization of element fluxes into lavas in the seafloor weathering zone

	a[1]	b[1]
CO_2	0.6(0.5)	0.11(0.03)
Na_2O	0.02(0.12)	-0.02(0.01)
SiO_2	0	-0.18(0.06)
CaO_{sil}	1.0(1.6)	-0.27(0.14)
K_2O	0	0.09(0.03)

[1]Flux (g yr^{-1}) = $10m(a + bT)$; where m = mass production rate of lavas that undergo seafloor weathering (kg yr^{-1}), T = bottom water temperature (°C).

Figure Captions

Fig. 1: Location map of the study area on the northern flank of the Troodos ophiolite and locations of the whole-rock, glass and carbonate samples. Drill core samples (CY1 and 1A) are projected to the surface to show their relative locations.

Fig. 2 Variation with depth in the Troodos ophiolite lavas (from left to right) of: (column 1) stratigraphy and dominant void filling secondary phases; (column 2) carbonate precipitation temperature; (column 3) whole rock CO_2; (column 4) whole rock K_2O; and (column 5) whole rock Na_2O. The well-ventilated region of the crust in each section is indicated by the blue horizontal shading. Temperatures of carbonate formation were calculated using the formulation of Epstein et al. (1953) and assuming a seawater $\delta^{18}O$ of -1‰ for an ice-free Cretaceous ocean. Using alternative formulations of the O-isotope thermometer could lead to temperatures 3-5°C higher (Coplen, 2007) or 2-4°C lower (Kim and O'Neill, 1997) which would not change the interpretations. Also shown in column 2 are conductive geotherms for 2 (180 mW m^{-2}) and 10 (80 mW m^{-2}) Myr old oceanic lithosphere (dashed orange lines; based on model of Hasterok, 2013) starting at the base of the well-ventilated region assuming a temperature of 15°C in this zone. This age range spans much of the time interval of mineral precipitation in off-axis hydrothermal systems with younger ages having larger geotherms. The histograms in the K_2O and Na_2O columns show the distribution of glass (i.e. protolith) compositions in this region (data from Supplementary Table S2 and Regelous et al., 2014). Row 1 (green): Mitsero; row 2 (blue) Akaki; row 3 (orange) Politico; and row 4 (black) Onophrious. Circles: pillows, Squares: sheets; Open: interior, Filled: rim; Filled diamonds: hyaloclastites; Open diamonds: unknown position in lava unit and/or lithology. Where olivine is present as a phenocryst it is generally <5% of the rock.

Fig. 3. Whole rock: (a) MgO versus silicate-hosted CaO (see text for details), and (b) TiO_2 versus SiO_2/Al_2O_3 showing the large-scale chemical changes in these elements in altered rocks relative to cogenetic volcanic glasses (i.e. protoliths; outlined in grey). Unknown: position in lava unit unknown.

Fig. 4. Compositional zoning across three pillows of different sizes (red, green and blue symbols) from the same outcrop (Fig. S1) and associated interpillow material (grey). The limited range of Al_2O_3/TiO_2 in the pillow samples (a) indicates these elements were largely immobile. Element abundances in (b) to (e) are normalized to a constant TiO_2 content (0.6 wt%; the average of all pillow analyses) to account for mass gain or loss. The protolith probably contained 10-12 wt% CaO, 1.5-2 wt% Na_2O, 8-9.5 wt% MgO; 51-53 wt% SiO_2 and 0.1 to 0.2 wt% K_2O (see later). The solid grey lines are regressions through the data and the dashed lines show bulk outcrop compositions based on spherical (model 1) and cylindrical (model 2) pillows as described in the text.

Fig. 5. Scatter plot of whole rock Ni and Cr contents showing that the vast majority of samples, whether olivine bearing (green symbols) or olivine free (blue symbols), show the same correlation of Cr and Ni, across the same range of Ni abundance, as in cogenetic glasses (red symbols). Brown symbols: samples from CY1/1a drill core that it is

unknown whether they were olivine-bearing or not. The greater scatter in the whole rock relative to glass samples probably represents minor olivine (and/or Cr-spinel) accumulation along with redistribution of Ni during alteration. The circled samples may contain accumulated olivine enriching them in Ni, even though olivine was not observed. Alternatively, they may have been enriched in Ni by hydrothermal processes. Two very olivine-rich samples (>600 ppm Ni) from the CY1 drill core (Gibson et al., 1991) are not shown here and were not used in this study. The red solid line is a regression through the glass data forced through the origin and the dashed lines show the impact of adding 2.5% and 5% olivine to this assuming a representative olivine-melt partition coefficient of 12 for Ni (e.g. Li and Ripley, 2010).

Fig. 6. Histograms of the change in sample compositions due to hydrothermal alteration for all samples from the different study areas in the Troodos ophiolite and all samples from the upper, well-ventilated, seafloor weathering zone (SFWZ) portion of the Troodos lavas (red). Probability distributions are shown for all the data as lines (black), data from well-ventilated areas (red), and data from poorly ventilated areas (blue dashed) all scaled to the total number of samples. The average and standard error for all data are shown as the header with the same for just samples from well-ventilated areas in parentheses.

Fig. 7 Calculated average changes in rock composition in the well-ventilated (seafloor weathering) zones of different sections of upper oceanic crust (Table 1; the unweighted data is used for the Troodos ophiolite) plotted as a function of average alteration temperature derived from carbonate O-isotope thermometry (Fig. 2, Fig. S6). Also shown in (f) are published CO_2 contents that include estimates of void filling carbonates (grey symbols and text; see text for details). The equations are linear fits through the data with uncertainties on parameter estimates in parentheses. For MgO two fits are shown including all data (blue) and excluding Hole 417A (brown) due to uncertainty in whether the large MgO loss in this core is representative. ΔCaO is the change in the silicate hosted CaO content of the rock.

Fig. 8 Estimates of the flux of major ions leached from lavas during seafloor weathering over the last 100 Myr based on the temperature dependencies given in Table 2 and the ocean bottom water temperature of Cramer et al. (2011). The models hold the crustal creation rate constant at 3.4 km^2 yr^{-1} and assumes an average 200 m thick seafloor weathering zone over all seafloor formed and a density of the seafloor weathering zone of 2500 kg m^{-3}. Fluxes are shown as if they occur instantaneously at the time of crustal accretion; in reality off-axis hydrothermal fluxes occur from crust of a range of ages and this would have the effect of generally smoothing the variability in flux somewhat. Estimates of the black smoker fluxes for Ca, Si and K are shown as dashed lines for comparison (Coogan and Dosso, 2012).

Figure 1

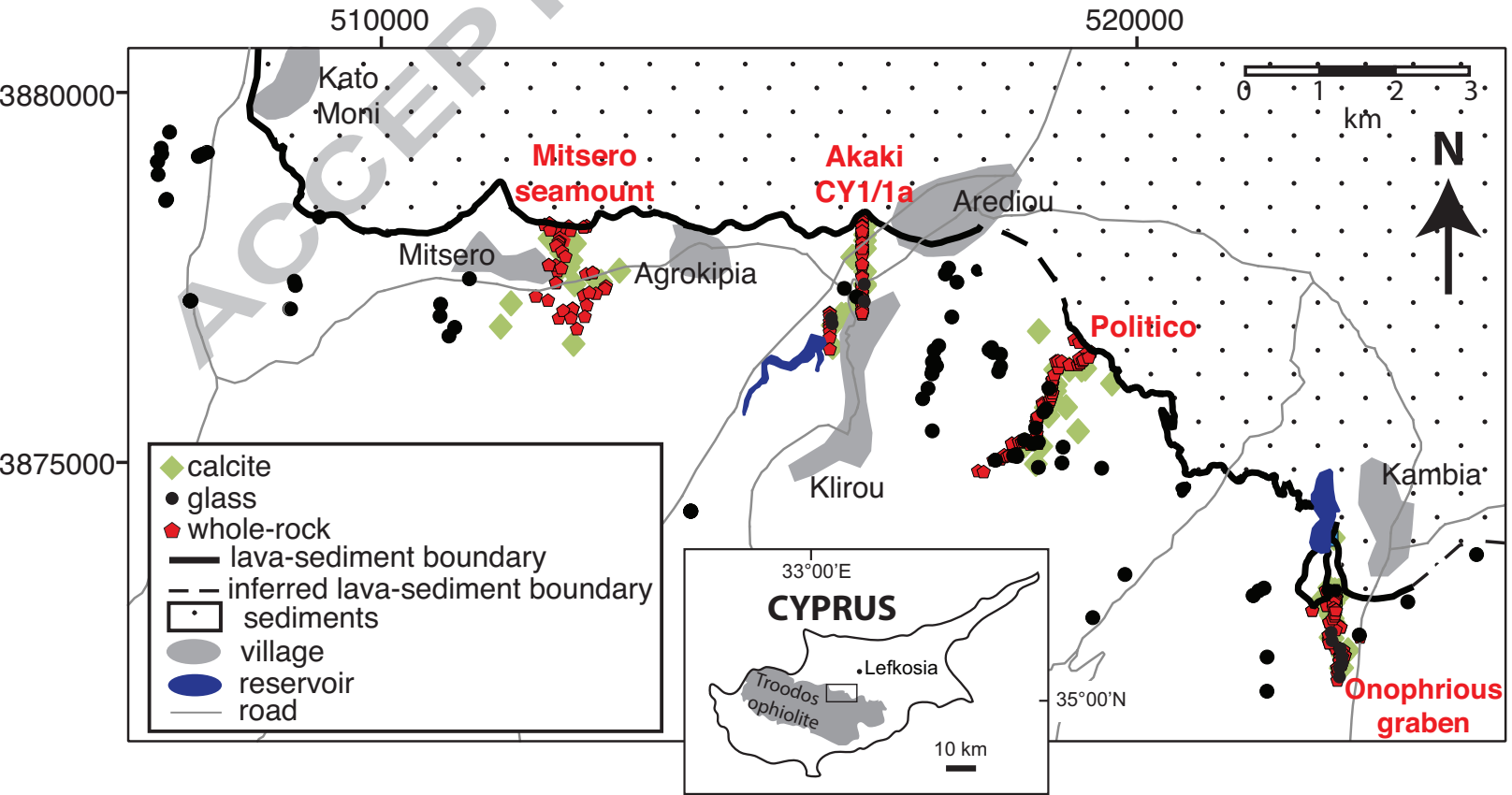

Figure 2

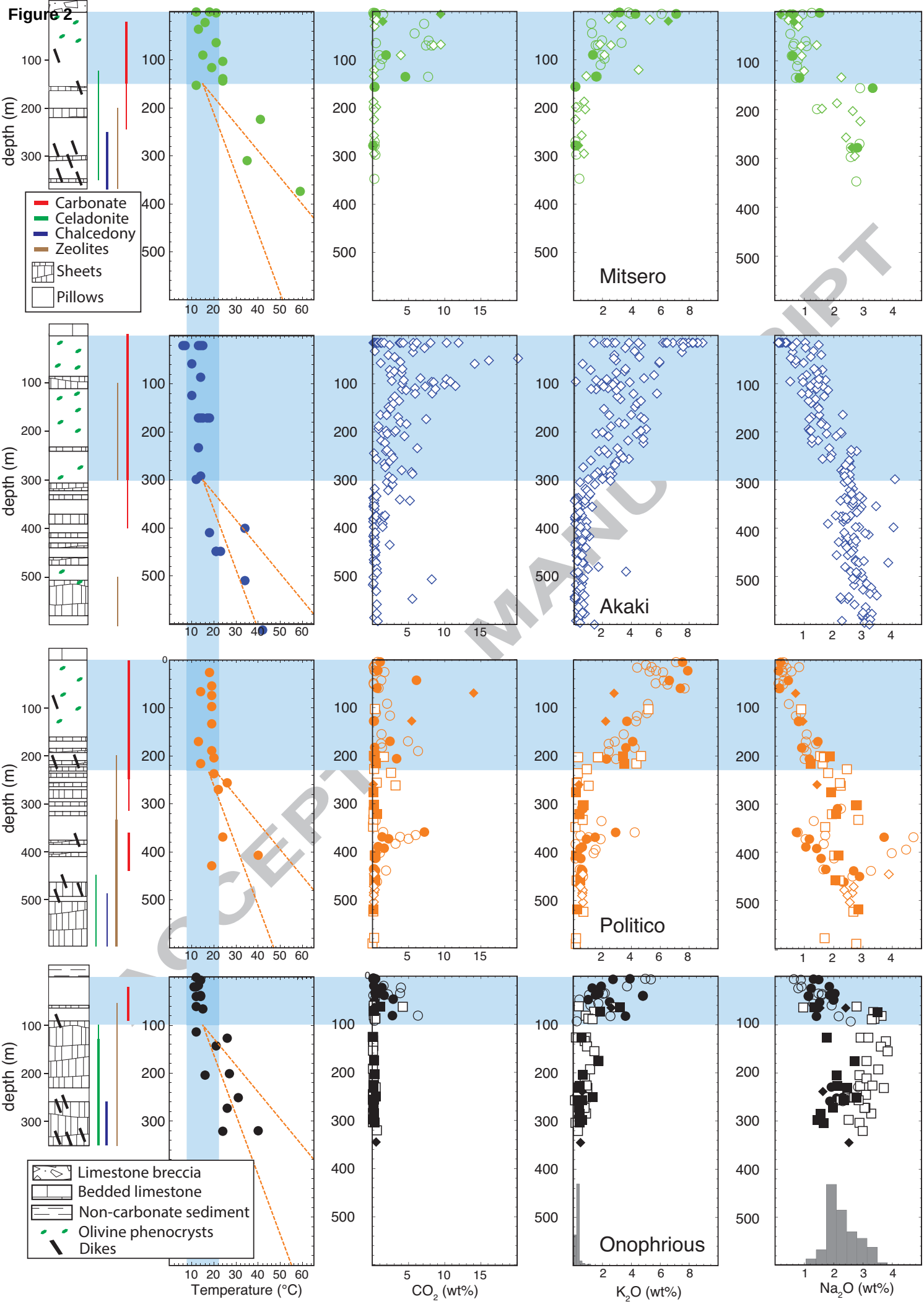

Figure 3

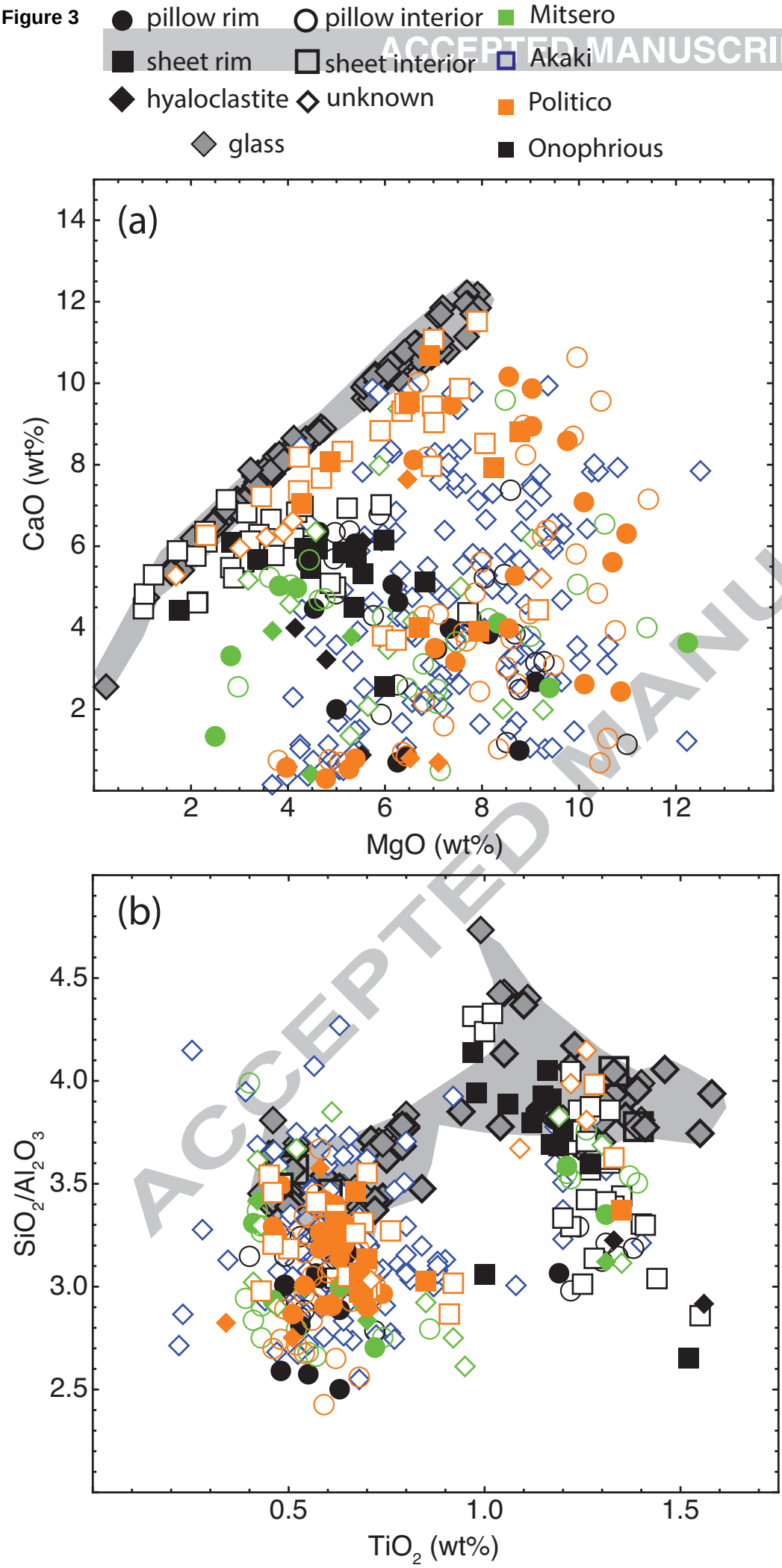

Figure 4

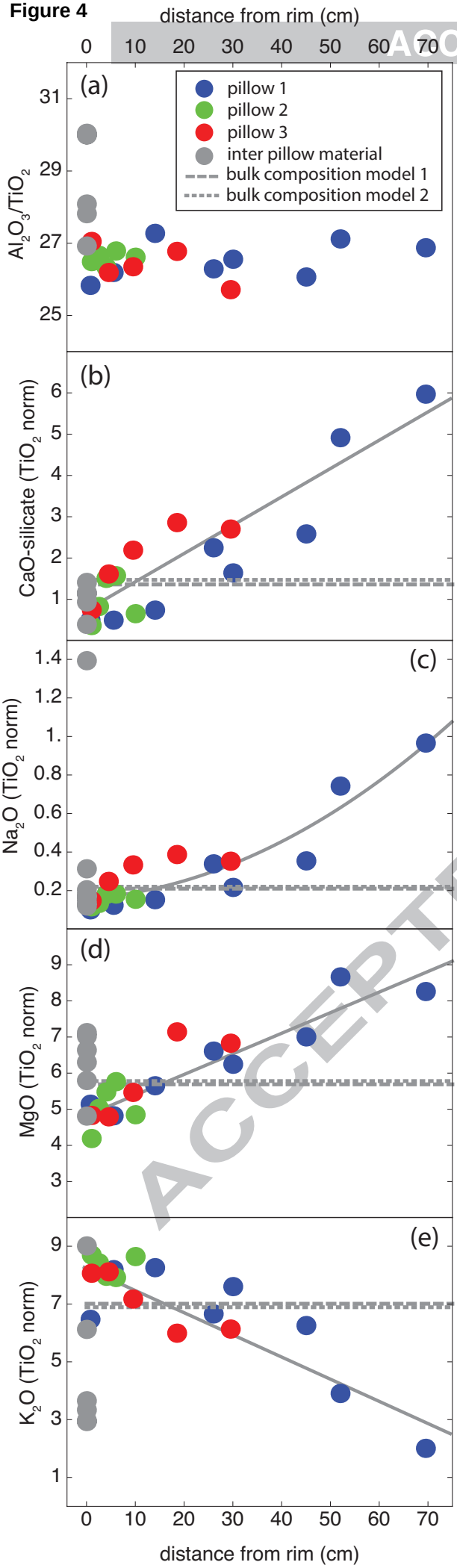

Figure 5

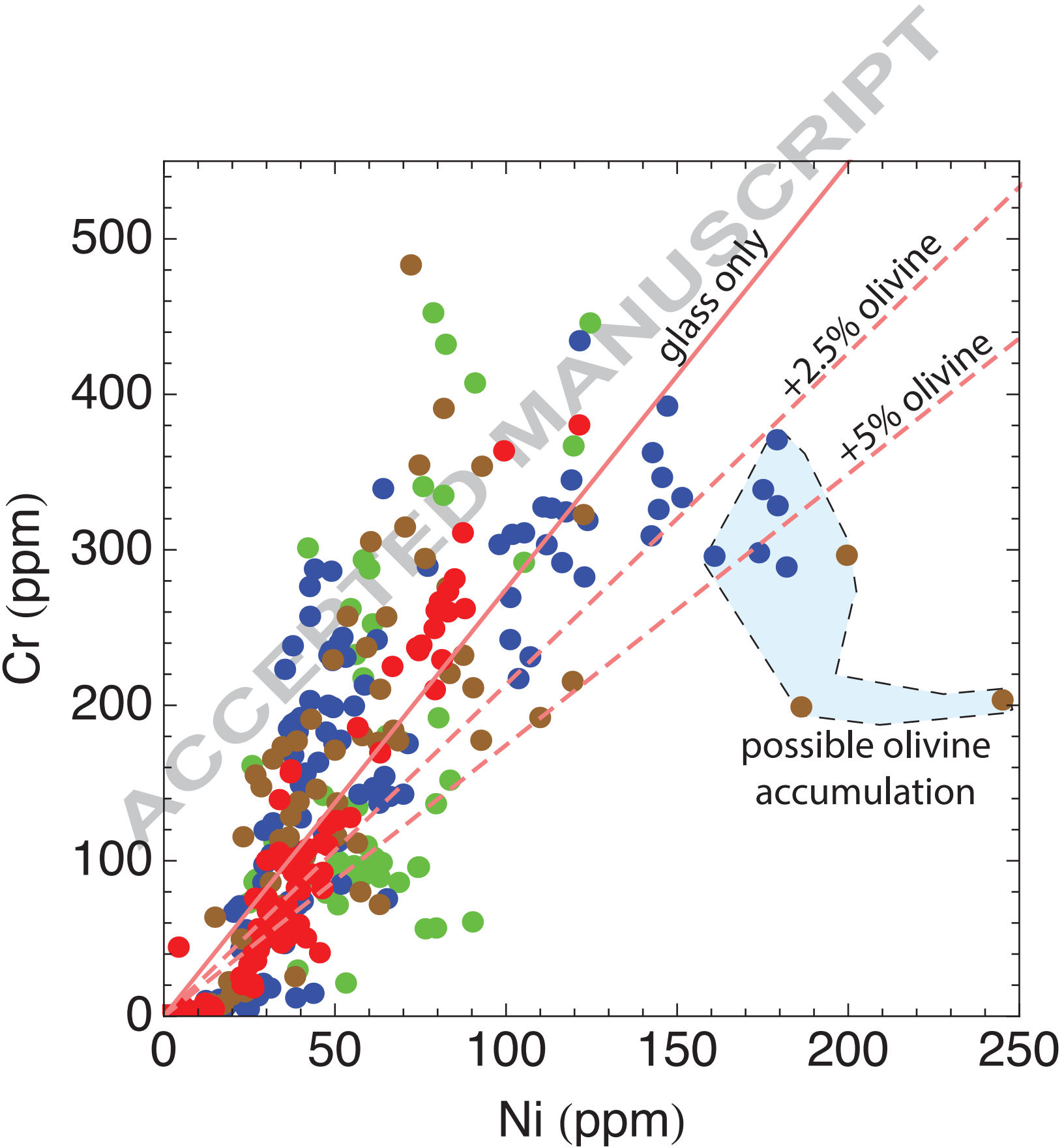

Figure 6

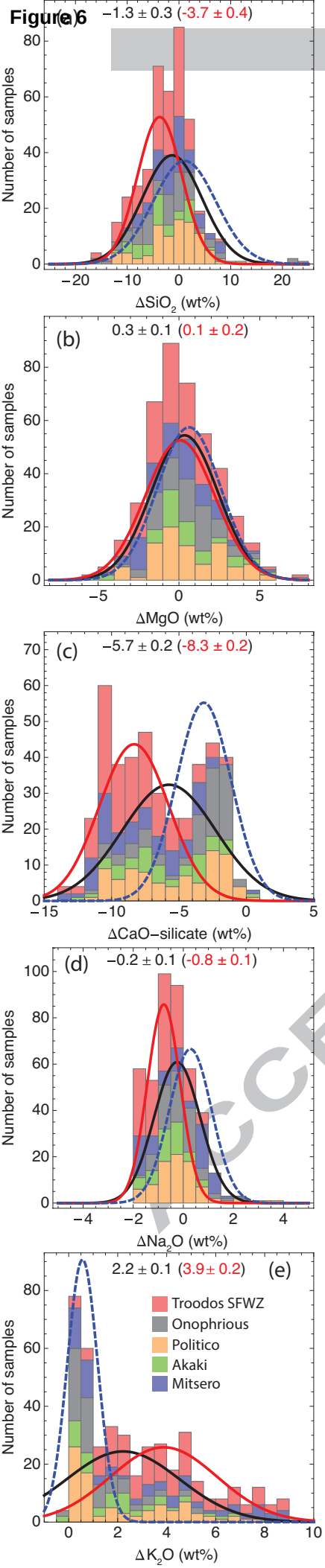

Figure 7

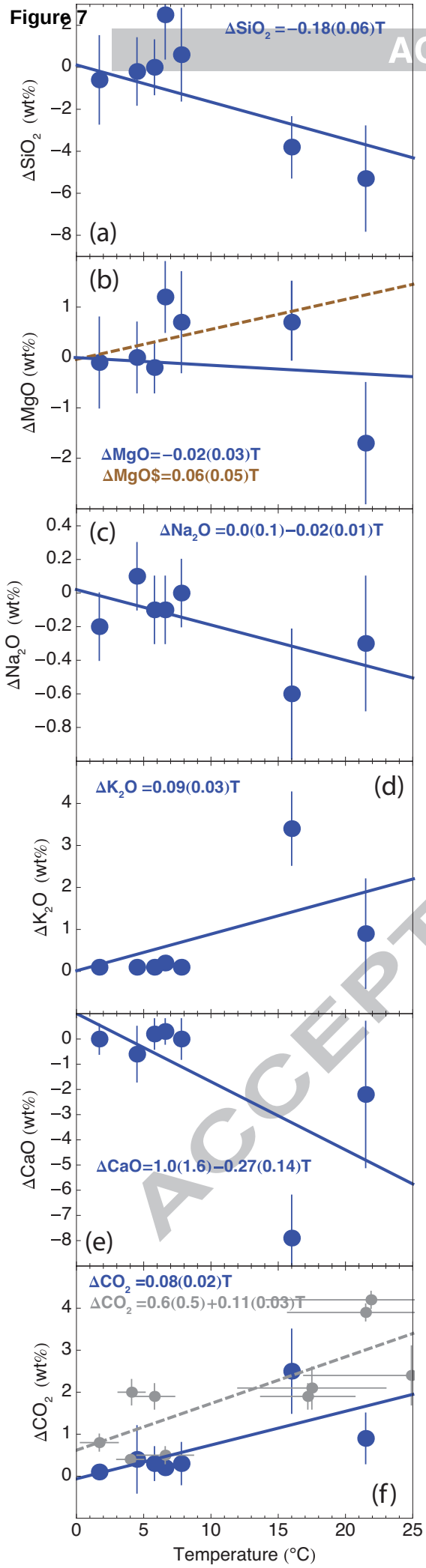

Figure 8